

See discussions, stats, and author profiles for this publication at: <https://www.researchgate.net/publication/231651506>

# Cooperative Phase Transformation in Self-Assembled Metal-on-Oxide Arrays

ARTICLE in THE JOURNAL OF PHYSICAL CHEMISTRY C · JANUARY 2009

Impact Factor: 4.77 · DOI: 10.1021/jp808695r

---

CITATIONS

7

---

READS

17

## 4 AUTHORS, INCLUDING:



**Giovanni Barcaro**

Italian National Research Council

106 PUBLICATIONS 1,601 CITATIONS

SEE PROFILE



**Alessandro Fortunelli**

Italian National Research Council

210 PUBLICATIONS 3,996 CITATIONS

SEE PROFILE



**Gaetano Granozzi**

University of Padova

301 PUBLICATIONS 4,396 CITATIONS

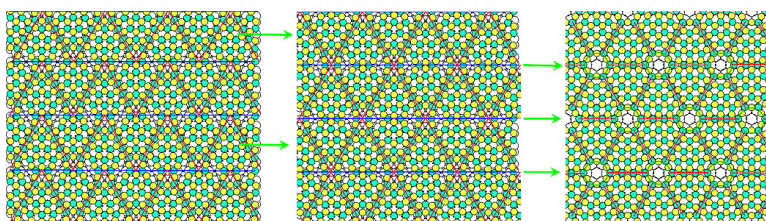
SEE PROFILE

## Cooperative Phase Transformation in Self-Assembled Metal-on-Oxide Arrays

Giovanni Barcaro, Alessandro Fortunelli, Gaetano Granozzi, and Francesco Sedona

*J. Phys. Chem. C*, **2009**, 113 (4), 1143-1146 • DOI: 10.1021/jp808695r • Publication Date (Web): 07 January 2009

Downloaded from <http://pubs.acs.org> on March 23, 2009



Phase transformation of a TiOx/Pt(111) film induced by Au deposition and heating

### More About This Article

Additional resources and features associated with this article are available within the HTML version:

- Supporting Information
- Access to high resolution figures
- Links to articles and content related to this article
- Copyright permission to reproduce figures and/or text from this article

[View the Full Text HTML](#)



ACS Publications  
High quality. High impact.

## Cooperative Phase Transformation in Self-Assembled Metal-on-Oxide Arrays

Giovanni Barcaro,<sup>†</sup> Alessandro Fortunelli,\* Gaetano Granozzi,<sup>‡</sup> and Francesco Sedona<sup>‡</sup>

IPCF-CNR, Via G. Moruzzi 1, Pisa, 56124, Italy, and Dip. di Scienze Chimiche, Università di Padova, Via Marzolo 1, Padova, 35131, Italy

Received: October 01, 2008; Revised Manuscript Received: December 11, 2008

The thermal behavior of a composite system formed by gold nanoclusters self-organized on a  $\text{TiO}_x/\text{Pt}(111)$  ultrathin film is investigated via first-principles simulations. A cooperative phase transformation from a rectangular to an hexagonal phase occurs at high temperature, by which Au clusters do not coalesce, but rearrange their shape and positions together with the more mobile regions of the oxide. A model describing the atomistic processes behind this transformation is proposed that is in full agreement with available experimental data.

Ultrathin oxide films grown on metal supports have recently attracted great attention as substrates for studying the growth and reactivity of metal deposits.<sup>1</sup> With respect to bulk systems, they offer the advantage of being conductive to some extent and thus can be characterized with atomistic resolution by electron-based probe techniques.<sup>2</sup> Moreover, especially in the case of polar films they are often modulated into regular nanostructured patterns opening up into point defects that act as trapping and nucleation centers<sup>3</sup> and thus constitute nearly ideal nanotemplates.<sup>4</sup> However, when employed as model catalysts their thermal stability becomes a central issue, especially when the reactions to be catalyzed are strongly exothermic (as in the case of CO and NO oxidation catalyzed by gold particles),<sup>5</sup> as the evolved heat can induce particle detachment from the substrate, Ostwald ripening and sintering<sup>6</sup> leading to larger particles and/or to the loss of beneficial particle-substrate interactions,<sup>7–9</sup> and thus to deactivation of the catalyst.<sup>10</sup> The presence of the underlying metal support makes ultrathin substrates promising in terms of heat dispersion, but their nanoscale dimension is likely to originate novel phenomena, such as structural phase transformations of both the metal aggregates and the oxide layer. Herein we show through static and dynamic density functional (DF) simulations on Au clusters self-assembled on a titanium oxide  $\text{TiO}_x/\text{Pt}(111)$  polar ultrathin film<sup>11,12</sup> that the combined effect of metal adsorption and heating induces a peculiar transformation from a metastable rectangular to a stable hexagonal phase without implying a detachment of the metal clusters from their trapping centers. This is the first example of a cooperative phase transformation in self-assembled metal-on-oxide arrays of interest from the point of view of basic science and also as it suggests that these systems can be robust enough to cross the gap between model studies and practical applications.

The atomistic structure of a polar ultrathin titanium oxide film grown on the  $\text{Pt}(111)$  surface (named  $z'$ -phase in ref 13) is

\* To whom correspondence should be addressed. E-mail: (A.F.) fortunelli@ipcf.cnr.it; (G.G.) gaetano.granozzi@unipd.it.

<sup>†</sup> IPCF-CNR.

<sup>‡</sup> Università di Padova.

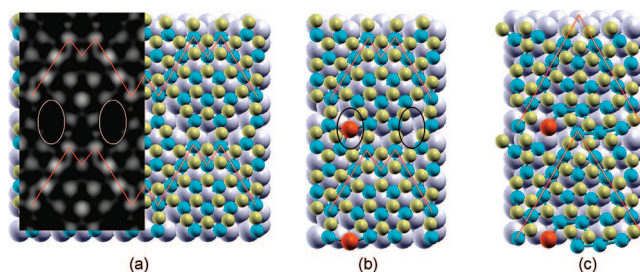


**Figure 1.** Atomistic structures of (a) the bare  $z'$ -phase at  $T = 0$  K; (b) the same phase with a Au atom adsorbed inside the defective hole at  $T = 0$  K; (c) the same system as in panel b, but now as a snapshot from a first-principles molecular dynamics simulation at  $T = 600$  K. Pt, Ti, O, and Au atoms are represented as gray, yellow, light blue, and red colors, respectively. In panel a, an STM image at 1 eV bias simulated using the Tersoff–Hamann approach<sup>21</sup> at a height of 2 Å above the oxygen layer is also shown. The defective holes are highlighted with white circles in (a) and as black circles in (b). The simulations used the PW91 xc-functional<sup>22</sup> and ultrasoft pseudopotentials<sup>23</sup>

schematically shown in Figure 1a, together with a simulated STM image at positive bias (1 eV).<sup>11</sup> This film is constituted of (i) compact pseudoepitaxial regions where triangular islands of oxygen-tricoordinated titanium atoms are separated by zigzag-like lines of oxygen-tetracoordinated titanium atoms (the latter appear brighter in the STM images at positive bias, hence the  $z'$  nomenclature), and (ii) defective troughs (appearing darker in the STM images) that are aligned along the  $\langle 1\bar{1}0 \rangle$  directions of the  $\text{Pt}(111)$  surface and are based on irregular  $\text{Ti}_2\text{O}_3$  units that alternate with Ti vacancies or “holes” (highlighted with white circles in Figure 1a) exposing the bare metal support.<sup>11</sup> In Figure 2a, an STM image of the  $z'$ -phase after the deposition of 0.9 monolayer equivalent (ML) of Au is displayed;<sup>14</sup> the Au clusters nucleating on the holes along the troughs of the  $z'$ -phase<sup>3</sup> are very regular with a narrow size distribution despite their small size (the average number of atoms is roughly estimated to be around 25) and grow along a preferential orientation, highlighted with black lines in Figure 2a. It can be noted that the shape of the smaller clusters is elongated in the direction of the preferential orientation. The cluster/oxide/metal

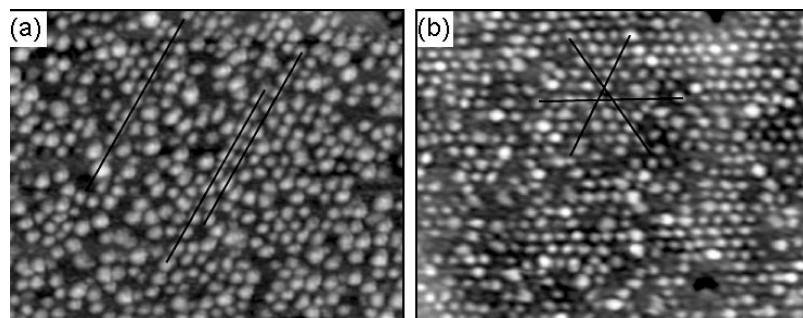


**Figure 2.** STM constant-current images of Au clusters deposited at 0.35 ML coverage on the  $z'$ - $\text{TiO}_x$  phase: (a) as deposited at  $T = 300$  K ( $50 \times 40$  nm<sup>2</sup>,  $V = 1$  V,  $I = 0.5$  nA); (b) after a postdeposition annealing in UHV at  $T = 600$  K for 15 min ( $50 \times 40$  nm<sup>2</sup>,  $V = 1$  V,  $I = 0.5$  nA).

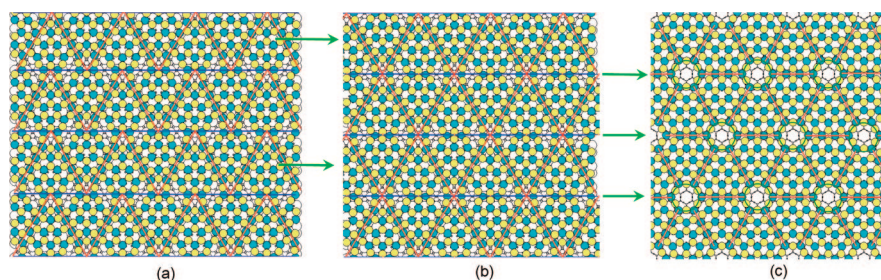


**Figure 3.** Schematic representation of the transformation from (a) the rectangular  $z'$ - $\text{TiO}_x$  /Pt(111) phase to (b) an intermediate (hexagonal)  $z'$ -phase with still two holes per cell, to (c) an hexagonal  $z'$ -phase with only one hole per cell and full  $p6m$  symmetry. Color convention as in Figure 1.

system is quite stable; no change is observed after annealing in UHV for several minutes at temperatures up to 550 K. However, at higher temperatures a peculiar phenomenon is observed, by which the rectangular pattern of nanoclusters transforms into an hexagonal one, and the transformation is almost complete above 600 K.<sup>12</sup> In Figure 2b, an STM image obtained after annealing at 600 K for 15 min is shown.<sup>14</sup> Note that there are now three preferential orientations, highlighted with black lines in Figure 2b. Moreover, the Au clusters are more spatially separated, even though their density is roughly constant, and their shape (also for the smaller clusters) is more rounded. This transformation has no counterpart in the pure titanium oxide phases and is only observed for the composite metal-on-oxide-on-metal system.<sup>15</sup>

In order to rationalize the mechanisms behind such a peculiar transformation, first-principles molecular dynamics (Car–Parrinello, CP)<sup>16</sup> simulations were conducted on the  $\text{TiO}_x$   $z'$ -phase both as a bare system and with a Au atom adsorbed inside the defective hole.<sup>17</sup> The  $z'$ -phase turned out to be thermally stable; CP runs were performed at  $T = 300$  K and at  $T = 600$  K, each one for a total time of 3–5 ps without any noticeable effect. An analogous result was obtained when a Au atom was adsorbed inside the hole and CP simulations were performed at  $T = 300$  K, as can be appreciated from Figure 1b, where a schematic picture of the optimized structure obtained after a local energy minimization (using the PWscf code) is shown.<sup>18</sup> On the contrary, when the temperature was raised to 600 K, the system rapidly rearranged to a different configuration, shown in Figure 1c as a representative snapshot taken from the corresponding CP run. The two defective holes along the troughs merged into a single one, while the zigzag-like motifs of oxygen-tetracoordinated titanium atoms deformed from a W-shape into a triangular outline. This structural transformation is a purely entropic effect; a local energy minimization starting from the configuration of Figure 1c brings the system back to the configuration of Figure 1b. Its driving force lies in the fact that

the Au atom is somewhat constrained in the hole,<sup>3</sup> and the associated tension increases with increasing kinetic energy of Au.

As cell dimensions and stoichiometry are held fixed in our simulations, a rectangular translational symmetry is imposed and the system is not free to relax to a different (e.g., hexagonal) periodicity. The structure shown in Figure 1c however is very suggestive. Note that the dimensions of the rectangular unit cell are such that the cell height (14.4 Å) is in a  $\sqrt{3}/2$  ratio with the cell width (16.6 Å), so that the arrangement shown in Figure 1c can be viewed as a pattern of horizontally disposed stripes of equilateral triangles (Figure 3a). Now, such a regular pattern can be transformed into an hexagonal arrangement by translating every second stripe by half an horizontal lattice parameter (Figure 3b). This new configuration is quite competitive; its energy per unit cell being only 0.42 eV higher than that of the rectangular structure at the DF level. Moreover, small displacements of the  $\text{Ti}_2\text{O}_3$  units in the troughs produce a merging of the two holes into a single one and create a perfect hexagonal arrangement (Figure 3c). This last structure is a local energy minimum (at variance with the kinetically stabilized configuration of Figure 1c), has hexagonal symmetry (cell edge 16.6 Å), presents merged equidistant holes, is thermally stable within the constraints given by its geometry, and is isoenergetic with the structure of Figure 3b. The interconversion shown in Figure 3 thus represents a route for the experimentally observed rectangular-to-hexagonal transformation, taking place via atomic rearrangements in the oxygen overlayer and along the troughs.

Both the rectangular (Figure 1a) and hexagonal (Figure 1c) cells were then used as templates for density functional basin-hopping (DF-BH) calculations of the structure and energetics of  $\text{Au}_N$  clusters ( $N = 1–8$ ) adsorbed on them (calculations on selected structures were also conducted up to  $\text{Au}_{11}$ ). The DF-BH approach is a first-principles global optimization method<sup>19</sup> that allows one to explore the potential energy surface of complex systems and predict their global minima.<sup>20</sup> The binding



**TABLE 1: Total Binding Energies of Au<sub>N</sub> Clusters on the Rectangular and Hexagonal Phases**

cluster	$E_{\text{bnd}}$ (rect)	$E_{\text{bnd}}$ (hex)
Au <sub>1</sub>	1.76	1.43
Au <sub>2</sub>	3.47	3.47
Au <sub>3</sub>	5.63	5.57
Au <sub>4</sub>	7.74	8.36
Au <sub>5</sub>	9.91	10.81
Au <sub>6</sub>	12.37	13.20
Au <sub>7</sub>	14.40	14.67
Au <sub>8</sub>	16.53	17.03

energies of the combined cluster/oxide/support systems from such calculations, i.e., the difference between the sum of the energies of the separated fragments in their equilibrium configurations (metal atoms in the gas-phase and supported titania film) and the energy of the composite system, are reported in Table 1. Note that the clusters on the rectangular phase are favored for few (up to three) Au atoms, but the situation is reversed for Au clusters with four or more atoms. The hexagonal metal-on-oxide phase thus become not only entropically but also *thermodynamically* more stable than the rectangular one, and this explains why this arrangement is maintained after the system is brought back to RT. The reasons for this energetic crossover lie in the better interaction of the Au clusters with the defective oxide surface in the hexagonal phase, obtained without sacrificing the cluster internal energy. It can be added that the clusters on the hexagonal phase have a more rounded aspect in agreement with experiment (Figure 2b). Even though computational limitations do not allow us to investigate clusters of the same size as in the experiments (the average number of atoms for the clusters of Figure 2 can be roughly estimated to be around 25 while we have tentative structures only up to Au<sub>11</sub>), we believe that the prediction of an energetic crossover between metal-on-oxide rectangular and hexagonal phases can be extrapolated to the experimentally investigated régime (further experiments are in progress to verify this point).

Note from Table 1 that the binding energies of the clusters to the substrate are substantial, so that cluster coalescence from detrapping is unlikely under the given experimental conditions. This statement can be substantiated by the following arguments. The energy differences involved in the (Au<sub>N</sub> → Au<sub>N-1</sub> + Au) fragmentation ( $N \geq 2$ ) for Au clusters adsorbed on the rectangular phase range between 2.03 and 2.46 eV (actually, it can be noted in passing that with the exception of Au<sub>6</sub> these energy differences range in a very narrow interval of 2.03/2.17 eV and that one does not observe the usual even-odd oscillations in the incremental formation energy of noble metal clusters).<sup>19</sup> Setting the adsorption of a single Au atom on the neighboring oxygen atoms to 0.2 eV<sup>3</sup> and even neglecting any additional energy penalty due to transition state rearrangements, the energy barriers for the fragmentation of a single Au atom can be roughly estimated to be at least  $\approx 1.83$  eV. By assuming an Arrhenius prefactor of  $\approx 10^{13}$  Hz (which is an upper bound to typical values), it turns out that fragmentation is predicted to occur on a time scale of hours. Ostwald ripening via single-atom fragmentation is thus unlikely for short (15 min) annealing even at 600 K. Fragmentation of larger species, such as a Au<sub>2</sub> dimer, can also be considered. Detachment of a dimer turns out to be more favorable than that of a single-atom, as in similar cases,<sup>19</sup> but still the corresponding energy barriers are predicted to be at least 1.6 eV (with the only exception of Au<sub>3</sub>, which suffers from the scarce stability of the Au dimer adsorbed on the hole of the z'-phase, and Au<sub>8</sub>, which suffers for the peculiar stability of the Au<sub>6</sub> cluster). Cluster sintering via disruption of

small clusters is thus not viable according to our calculations under the given experimental conditions, in fair agreement with the experimental result that the dimensions of the Au clusters are not strongly perturbed by the annealing process.<sup>12</sup>

In conclusion, metal-on-ultrathin-oxide systems present a great potential interest in several fields, including heterogeneous catalysis, as the oxide acts as a protective layer, hindering alloying of metal particles with metal of the support, while the steric constraints and the electrostatic field generated by the charge-separated layer can trap metal atoms (surface nanopatterning) and orient the cluster growth into ordered metal arrays, in addition to originating novel phenomena. Given the nanoscale dimensions of the interface and the exothermal character of many catalytic processes, the thermal stability of these materials is a key issue. The present analysis unveils the atomistic processes behind the first example of a cooperative phase transformation in such systems, by which regular Au/TiO<sub>x</sub>/Pt(111) arrays transform from a metastable rectangular to an hexagonal phase. This transformation is favored by both entropic and energetic factors, and occurs without cluster detrapping or alloying with the support, but via a rearrangement of their shapes and positions together with the more mobile and defective regions of the oxide to increase their relative distance and optimize cluster/substrate interactions. Given the growing activity in this field, the present results are expected to be followed by more such examples in the future.

**Acknowledgment.** We thank the DEISA Consortium (co-funded by the EU, FP6 project 508830) for support within the DEISA Extreme Computing Initiative ([www.deisa.org](http://www.deisa.org)) and for providing CPU time on the CSC supercomputing center. Carlo Cavazzoni and Paolo Giannozzi are gratefully acknowledged for porting the PWscf and CP codes and improving scalability for CPU and RAM requirements.

## References and Notes

- (1) Freund, H.-J. *Surf. Sci.* **2007**, *601*, 1438–1442.
- (2) Sterrer, M.; Fischbach, E.; Risse, T.; Freund, H.-J. *Phys. Rev. Lett.* **2005**, *94*, 186101.
- (3) Barcaro, G.; Fortunelli, A.; Granozzi, G. *Phys. Chem. Chem. Phys.* **2008**, *10*, 1876, and references therein.
- (4) Hamm, G.; Becker, C.; Henry, C. R. *Nanotechnology* **2006**, *17*, 1943.
- (5) Hutchings, G. J.; Haruta, M. *Appl. Catal., A* **2005**, *291*, 1.
- (6) Parker, S. C.; Campbell, C. T. *Top. Catal.* **2007**, *44*, 3–13.
- (7) Yoon, B.; Hakkinen, H.; Landman, U.; Wörz, A. S.; Antonietti, J.-M.; Abbet, S.; Judai, K.; Heiz, U. *Science* **2005**, *307*, 403–407.
- (8) Chen, M. S.; Goodman, D. W. *Top. Catal.* **2007**, *44*, 41–47.
- (9) Matthey, D.; Wang, J. G.; Wendt, S.; Matthiesen, J.; Schaub, R.; Laegsgaard, E.; Hammer, B.; Besenbacher, F. *Science* **2007**, *315*, 1692–1696.
- (10) Goguet, A.; Burch, R.; Chen, Y.; Hardacre, C.; Hu, P.; Joyner, R. W.; Meunier, F. C.; Mun, B. S.; Thompson, A.; Tibiletti, D. *J. Phys. Chem. C* **2007**, *111*, 16927–16933.
- (11) Sedona, F.; Granozzi, G.; Barcaro, G.; Fortunelli, A. *Phys. Rev. B* **2008**, *77*, 115417.
- (12) Sedona, F.; Agnoli, S.; Fanetti, M.; Kholmanov, I.; Cavaliere, E.; Gavioli, L.; Granozzi, G. *J. Phys. Chem. C* **2007**, *111*, 8024–8029.
- (13) Sedona, F.; Rizzi, G. A.; Agnoli, S.; Xamena, F. X. L. I.; Papageorgiou, A.; Ostermann, D.; Sami, M.; Finetti, P.; Schierbaum, K.; Granozzi, G. *J. Phys. Chem. B* **2005**, *109*, 24411.
- (14) The pictures reported in Figure 2 were obtained during the same STM experiments reported in ref 12 to which the reader is referred to for more details. The TiO<sub>x</sub> film was prepared by reactive deposition in the presence of oxygen ( $p_{\text{O}_2} = 10^{-4}$  Pa) and successive annealing in UHV at 673 K.<sup>11</sup> Au was evaporated from a filament basket on the TiO<sub>x</sub> substrate held at RT under UHV with a typical deposition rate of about 0.3 ML/minute. The sample preparation and characterization was performed using an OMICRON STM UHV system with a base pressure  $< 5 \times 10^{-9}$  Pa. STM images were obtained in constant current mode at RT.

(15) In ref 12, this transformation was interpreted as into a different  $w$ -TiO<sub>2</sub>/Pt(111) phase; the present analysis supersedes this previous hypothesis.

(16) Car, R.; Parrinello, M. *Phys. Rev. Lett.* **1985**, *55*, 2471.

(17) The CP calculations were performed using the ESPRESSO software (<http://www.quantum-espresso.org>). The time step was set to 25 au, the electron mass 3500 au, a CP run consisted of 500 minimization steps, 200 MD steps starting with null velocities at 300 K, and a variable number of production MD steps at the chosen temperature for a total simulation time between 3 and 5 ps using a Nosè thermostat for the kinetic energy of the electronic wave function. The CP runs were conducted at the Cray XT4 supercomputer of CSC (<http://www.csc.fi>) in Espoo, Finland.

(18) The PWscf (<http://www.pwscf.org>) calculations used ultrasoft pseudopotentials, the PW91 exchange-correlation functional,<sup>22</sup> and the following computational parameters (identical to those used in ref 3): 30 Ryd for the energy cutoff on the wave function, 150 Ryd for the energy cutoff on the electronic density, about 8–10 Å of empty space between atoms in replicated cells, a (2,2,1)  $k_{\text{mesh}}$  grid for the sampling of the first Brillouin zone, and 2 layers of Pt for describing the metal support.

(19) Barcaro, G.; Aprà, E.; Fortunelli, A. *Chem.—Eur. J.* **2007**, *13*, 6408–6418.

(20) The DF-BH method is based on a basin-hopping algorithm for the exploration of the potential energy surface combined with a density-functional method for the calculation of energies and forces. Each BH run starts with a randomly chosen atomic configuration and is composed of a given number of Monte Carlo steps. In each of these, the starting configuration is first locally optimized to obtain an energy  $E_1$ , then subjected to a random displacement of all the atoms up to  $\pm 1$  Å in each Cartesian coordinates, and finally locally optimized to obtain a new energy  $E_2$ . If  $\exp[(E_1 - E_2)/k_B T] > \text{rndm}$ , where rndm is a random number (Metropolis criterion), the new configuration is accepted; otherwise the old configuration is kept and the process is iterated. For each size, we performed three to five BH runs, each one composed of about 10–15 Monte Carlo steps, using a value of 0.5 eV as  $k_B T$  in the Metropolis criterion.

(21) Tersoff, J.; Hamann, D. R. *Phys. Rev. Lett.* **1983**, *50*, 1998–2001.

(22) Perdew, J. P.; Chevary, J. A.; Vosko, S. H.; Jackson, K. A.; Pederson, M. R.; Singh, D. J.; Fiolhais, C. *Phys. Rev. B* **1992**, *46*, 6671–6687.

(23) Vanderbilt, D. *Phys. Rev. B* **1990**, *41*, 7892–7895.

JP808695R